

The Structural Basis for the Selectivity of Benzotriazole Inhibitors of PTP1B[†]

Giovanna Scapin,^{*,‡} Sangita B. Patel,[‡] Joseph W. Becker,[‡] Qingping Wang,[§] Caroline Despons,[§] Deena Waddleton,[§] Kathryn Skorey,[§] Wanda Cromlish,[§] Christopher Bayly,[#] Michel Therien,[#] Jacques Yves Gauthier,[#] Chun Sing Li,[#] Cheuk K. Lau,[#] Chidambaram Ramachandran,[§] Brian P. Kennedy,[§] and Ernest Asante-Appiah[§]

Department of Medicinal Chemistry, Merck Research Laboratory, P. O. Box 2000, Rahway, New Jersey 07065, and Departments of Biochemistry & Molecular Biology and of Medicinal Chemistry, Merck Frosst Center for Therapeutic Research, P. O. Box 1005, Pointe-Claire - Dorval, Quebec, H9R 4P8, Canada

Received June 26, 2003; Revised Manuscript Received August 4, 2003

ABSTRACT: Protein tyrosine phosphatase 1B (PTP1B) has been implicated in the regulation of the insulin signaling pathway and represents an attractive target for the design of inhibitors in the treatment of type 2 diabetes and obesity. Inspection of the structure of PTP1B indicates that potent PTP1B inhibitors may be obtained by targeting a secondary aryl phosphate-binding site as well as the catalytic site. We report here the crystal structures of PTP1B in complex with first and second generation aryl difluoromethylphosphonic acid inhibitors. While all compounds bind in a previously unexploited binding pocket near the primary binding site, the second generation compounds also reach into the secondary binding site, and exhibit moderate selectivity for PTP1B over the closely related T-cell phosphatase. The molecular basis for the selectivity has been confirmed by single point mutation at position 52, where the two phosphatases differ by a phenylalanine-to-tyrosine switch. These compounds present a novel platform for the development of potent and selective PTP1B inhibitors.

Reversible tyrosine phosphorylation, controlled by protein tyrosine kinases and protein tyrosine phosphatases, plays a critical role in the transduction of signals that control many diverse processes, including passage through the cell cycle, proliferation and differentiation, metabolism, cytoskeletal organization, neuronal development, and immune response (for reviews see refs 1–4). Protein tyrosine phosphatases (PTPases) constitute a large, structurally diverse family of receptor-like and cytoplasmic enzymes expressed in all eukaryotes. The most recent reports indicate that there are about 60 PTPase genes encoded within the human genome, including transmembrane, receptor-like, and intracellular, nonreceptor-like enzymes. Each PTPase is composed of at least one conserved domain characterized by a unique 11-residue sequence motif ((I/V)HCXAGXXR(S/T)G) containing the cysteine and arginine residues known to be essential for catalytic activity. The diverse structures of PTPases result primarily from the variety of noncatalytic sequences attached at the carboxy- or amino-termini of the catalytic domain.

PTP1B¹ was the first PTPase to be isolated in homogeneous form (5, 6), crystallized, and have its tertiary structure determined (7). Since then, a number of biological, structural, and enzyme kinetic studies on PTP1B have suggested that it is an important negative regulator of the insulin-signaling pathway. Recent studies on PTP1B knockout mice (8, 9) provided significant support for the view that PTP1B is a key regulator of insulin signaling. PTP1B^{−/−} mice showed increased insulin sensitivity and obesity resistance, demonstrating that PTP1B plays a major role in modulating both insulin sensitivity and fuel metabolism. Thus, PTP1B is an attractive target for the treatment of type 2 diabetes and obesity, and selective PTP1B inhibitors could be of significant therapeutic utility (10).

Several groups have reported structurally diverse PTP1B inhibitors (for review see refs 11–13) that show a high degree of selectivity for PTP1B over several PTPases, including PTPα, LAR, CD45, and VHR, but generally not over the T-cell protein tyrosine phosphatase (TCPTP). Despite its name, TCPTP is a ubiquitous enzyme originally isolated from a human peripheral T-cell DNA library (14). The TCPTP cDNA encodes a 45-kDa protein (TC45) that displays 65% sequence identity overall and 72% identity within the conserved catalytic domain with PTP1B (15). TCPTP-deficient mutant mice exhibit specific defects in bone marrow stromal cells, B-cell lymphopoiesis, and erythro-

[†] The facilities at IMCA-CAT are supported by the companies of the Industrial Macromolecular Crystallography Association through a contract with Illinois Institute of Technology (IIT), executed through IIT's Center for Synchrotron Radiation Research and Instrumentation. Use of the Advanced Photon Source was supported by the U. S. Department of Energy, Basic Energy Sciences, Office of Science, under Contract No. W-31-109-Eng-38.

* To whom correspondence should be addressed. E-mail: giovanna_scapin@merck.com.

[‡] Merck Research Laboratory.

[§] Department of Biochemistry & Molecular Biology, Merck Frosst Center for Therapeutic Research.

[#] Department of Medicinal Chemistry, Merck Frosst Center for Therapeutic Research.

¹ Abbreviations: PTP-1B, phosphotyrosine phosphatase 1B; TC-PTP, T cell protein tyrosine phosphatase; PCR, polymerase-chain reaction; FDP, fluorescein diphosphate; DMH, *N,N'*-dimethyl-*N,N'*-bis(mercaptoacetyl)-hydrazine; MPD, methylpentanediol; F₂PMP, difluorophosphonomethyl phenylalanine; pTyr, phosphotyrosine; RMSD, root-mean-square deviation.

poiesis, as well as impaired T and B cell functions (16). These studies suggest that TCPTP plays a significant role in both hematopoiesis and immune function, and indicate that a therapeutically useful PTP1B inhibitor should display significant selectivity over TCPTP. The structures of PTP1B in complex with phosphotyrosine (17) and with a peptide derived from the insulin receptor (18) revealed a PTP1B specific second aryl-phosphate binding site adjacent to the catalytic site. The recently determined crystal structure of TCPTP shows that it also has primary and secondary aryl binding sites that are nearly identical to those in PTP1B (15). Nevertheless, small differences can be found around the secondary aryl binding sites, and PTP1B inhibitors that bind there may therefore be expected to achieve some degree of selectivity between the two enzymes. Attempts to design compounds that bind simultaneously to both sites resulted in the generation of several classes of inhibitor containing two pTyr mimetics. However, in all cases, crystallographic studies revealed a mode of binding that does not involve this second site (19–22). Recently, novel bidentate inhibitors, discovered by using a linked-fragment strategy, have been reported (23, 24). Crystallographic analysis shows that these inhibitors bind to both primary and secondary aryl binding sites, and that show moderate (up to 5-fold) selectivity for PTP1B over TCPTP. However, none of these compounds interact directly with any residues that differ between TCPTP and PTP1B, so the structural basis for the observed selectivity is not clear. The authors of this work speculate that the nearby differing residues may affect how these compound interact with the conserved residues Arg24 and Met258 (19).

Recently, a number of mono- or bis(aryldifluoromethylphosphonic acids) have been prepared in our laboratories, and shown to be potent PTP1B inhibitors with a good selectivity profile against other PTPs except TCPTP (Dufresne et al., in preparation; Lau et al., in preparation). A subsequent structure-based drug development based on the crystal structures of these first generation compounds, produced second generation inhibitors that resulted in selective inhibitors (Lau et al., in preparation). We report here the crystal structures of PTP1B in complex with these first and second generation compounds. These inhibitors represent a new class of ligands that interact with both the catalytic and secondary binding sites, and provide a moderate degree of selectivity for PTP1B over TCPTP. From the structural analysis, a potential selectivity determinant that differs between PTP1B and TCPTP and interacts directly with the selective inhibitors was identified. The appropriate mutant enzymes were constructed, and the pattern of their inhibition by these compounds confirms the structural analysis. We have also identified a novel, previously unexploited binding pocket, which may also help confer increased selectivity. The characterization and detailed understanding of the mode of binding of these compounds afford a novel platform for the design of improved potent and selective PTP1B inhibitors.

EXPERIMENTAL PROCEDURES

Mutagenesis and Protein Expression. Plasmids that express the isolated catalytic domains of human PTP1B(1–298) and TCPTP(1–296) were used as template DNA for the mutagenesis. Construction of the expression vectors has been described previously (25). The Phe52-to-Tyr and Tyr54-to-

Phe substitutions in PTP1B and TCPTP, respectively, were introduced using a PCR-based approach by following established protocols (26). Oligonucleotides used for the site-directed mutagenesis were custom synthesized by Research Genetics (Huntsville, AL). Codons specifying the targeted amino acid changes were incorporated into the mutant oligonucleotide primers as follows (the codon changes that were introduced have been underlined): F52Y (forward) – 5' AGAGACGTCAGTCCCTACGACCATAGTCGGATT 3'; F52Y(reverse) – 5' AATCCGACTATGGTCGTAGG-GACTGACGTCTCT 3'; Y54F (forward) – 5' AGAGAT-GTAAGCCCATTTCGATCACAGTCGTGTT 3'; Y54F (reverse) – 5' AACACGACTGTGATCGAATGGGCTTAC-ATCTCT 3'. The correct construction of the mutant derivatives was verified by DNA sequencing. DNA was subsequently isolated from positive clones and introduced into *Escherichia coli* BL21 cells for protein expression.

Protein Purification and Inhibitor Assays. The FLAG-tagged catalytic domain of PTP1B (residues 1–298) and TCPTP (residues 1–296) were expressed in *E. coli* and purified as reported previously (25, 27).

Activity Assays. The activity of PTP1B enzymes was assayed with fluorescein diphosphate (FDP) as substrate as reported previously (28). Briefly, the assays were carried out in a 96-well plate at room temperature in a buffer that consisted of 20 mM Bis-Tris, 5 mM DMH, 2 mM EDTA, 5% (v/v) DMSO, 2% (v/v) glycerol, 0.01% (v/v) Triton X-100 at a pH of 6.3. Hydrolysis of FDP was monitored continuously on a Cytofluor microplate reader with excitation and emission wavelengths set at 440 and 515 nm, respectively. Concentrations of PTP1B inhibitors that resulted in 50% reduction of enzyme activity (IC_{50}) were derived by fitting reaction rates obtained in the presence and absence of compounds to a 4-parameter equation using GraFit 4.0.10 (Erithacus Software). A substrate concentration equivalent to the K_M value for FDP was used for IC_{50} determinations. The concentration of each PTPase used for the determination of IC_{50} values was adjusted to achieve 10 arbitrary fluorescence units/s with respect to FDP hydrolysis.

Synthesis of Inhibitors. The methods for the synthesis of compounds will be published elsewhere (Lau et al., in preparation).

Protein Crystallization and Data Collection. All samples used for crystallization trials were routinely analyzed by light scattering using a Protein Solutions DynaPro instrument with Dynamics Version 4 software. The protein concentration was 10 mg/mL (i.e., the same concentration used for crystallization experiments); measurements were conducted at 20 ± 1 °C in 20 mM Tris/HCl, 5 mM DMH, 0.2 mM EDTA, 25 mM NaCl at a pH of 7.6. Crystals of PTP1B in complex with the compounds described in the text were obtained at 4 °C in hanging drops formed by mixing 1 μ L of protein solution (preincubated for 2 h at 4 °C with a 5-fold excess inhibitor) with 1 μ L of precipitant solution (12–18% PEG 4000, 200 mM $MgCl_2$, 100 mM HEPES, pH = 7.0). All data sets were collected at 100 K using synchrotron radiation at beamline 17-ID in the facilities of the Industrial Macromolecular Crystallography Association Collaborative Access Team (IMCA-CAT) at the Advanced Photon Source (Argonne National Laboratory, Argonne, IL). Crystals were dipped for about 10 s in cryoprotectant (15% MPD in mother liquor) before vitrifying them in the cryogenic nitrogen gas

Table 1: Statistics for the Processed Data for the Complexes of PTP1B with Compounds **2**, **3**, **4**, **6**, **9**, and **11**^a

compound	2	3	4	6	9	11
space group	<i>P</i> ₄ ₁ ₂ ₁ ²	<i>P</i> ₄ ₁ ₂ ₁ ²	<i>P</i> ₂ ₁ ₂ ₁	<i>P</i> ₂ ₁ ₂ ₁	<i>P</i> ₂ ₁ ₂ ₁	<i>P</i> ₂ ₁ ₂ ₁
UCP (Å)	<i>a</i> = <i>b</i> = 86.84, <i>c</i> = 139.69	<i>a</i> = <i>b</i> = 86.98, <i>c</i> = 139.83	<i>a</i> = 86.88, <i>b</i> = 88.41, <i>c</i> = 139.22	<i>a</i> = 87.95 <i>b</i> = 88.04, <i>c</i> = 139.23	<i>a</i> = 87.86 <i>b</i> = 87.76, <i>c</i> = 138.12	<i>a</i> = 88.03 <i>b</i> = 87.83, <i>c</i> = 138.93
molecules/AU	1	1	2	2	2	2
resolution range (Å)	37.0–2.2 (2.3–2.2)	37.0–2.2 (2.3–2.2)	37.0–2.1 (2.2–2.1)	20.0–2.3 (2.4–2.3)	20.0–2.2 (2.3–2.2)	28.0–2.3 (2.4–2.3)
no. of reflections	26131 (4348)	27955 (4547)	61938 (10233)	48690 (8039)	54806 (9032)	48228 (7902)
redundancy	8.7 (9.0)	8.0 (8.6)	3.5 (3.6)	7.1 (7.3)	7.1 (7.1)	5.6 (5.9)
completeness (%)	93.8 (93.0)	98.9 (100)	99.3 (100)	99.8 (100)	99.8 (100)	99.3 (99.1)
<i>I</i> / <i>σ</i> <i>I</i>	12.4 (2.2)	13.0 (2.9)	10.1 (2.5)	9.3 (1.5)	11.7 (3.2)	11.8 (2.1)
<i>R</i> _{sym} (<i>I</i>)	8.4 (40.4)	8.9 (40.7)	8.4 (38.2)	8.3 (38.2)	6.2 (21.2)	5.8 (32.4)

^a All data refer to reflections with *I*/*σ**I* greater than -3σ ; number in parentheses refer to data in the highest shell of resolution.

Table 2: Refinement Statistics for the Complexes of PTP1B with Compounds **2**, **3**, **4**, **6**, **9** and **11**

compound	2	3	4	6	9	11
resolution range (Å)	25.0–2.2	25.0–2.2	25.0–2.1	15.0–2.3	20.0–2.2	12.0–2.3
completeness (%)	91.2	98.4	94.2	96.1	97.1	97.4
no. of reflections work ^a	23623	26102	56665	44304	49422	44526
no. of reflections test ^a	1776	1379	2881	2341	3814	4167
<i>R</i> _{free} / <i>R</i> factor	24.5/21.5	24.6/21.0	23.8/20.8	23.8/21.0	23.3/19.6	24.6/21.4
RMSD bond length/angles (Å, degrees)	0.013/1.49	0.013/1.51	0.014/1.53	0.010/1.35	0.013/1.42	0.011/1.40
no. protein atom	2350	2350	4692	4692	4692	4697
No. solvent atoms	116	115	239	209	397	205
No. heteroatoms ^b	44	46	92	95	110	118

^a Work refers to reflections used during refinement; test to reflections set aside for *R*_{free} calculation. ^b Heteroatoms include ligand atoms and ions (if present).

stream. The crystals diffracted to 2.2–2.4 Å. Data were processed and scaled using X-GEN (29). Analysis of pseudo-precession photographs showed that crystals of the PTP1B/compound **2** and PTP1B/compound **3** complexes were tetragonal, space group *P*₄₁₂₁² or *P*₄₃₂₁², with one molecule per asymmetric unit (AU). Crystals of the complexes of PTP1B with compounds **4**, **6**, **9**, and **11** were orthorhombic, space group *P*₂₁₂₁, with two molecules per AU. Table 1 summarizes the statistics for the processed data.

Structure Solution and Refinement. The structure of PTP1B in complex with compound **3** (tetragonal space group) was solved by molecular replacement procedures using the software AMORE (30) and the protein coordinates from IPTY (17) as a searching model. A single solution was found that had a correlation coefficient of 51.5% and R-factor of 41.8% for data between 8 and 4 Å, and assigned the correct space group as *P*₄₁₂₁². The starting model was subjected to 30 cycles of rigid body refinement, followed by simulated annealing refinement (31, 32), using XPLOR version 3.843 with data between 8.0 and 3.0 Å; 5% of the data were flagged for R-free (33). The resulting model had a crystallographic R-factor of 27.6% (R-free was 42.6%), and inspection of difference Fourier electron density maps clearly showed the presence of the bound inhibitor. Alternating cycles of manual rebuilding of the model and computer-based methods using XPLOR was employed during refinement. The resolution was slowly increased to include all available data to 2.2 Å. The last few cycles of refinement were run using torsion angle dynamics (34), and positional and temperature factor refinement as implemented in CNX (Accelrys, San Diego, CA (35)). The structure of PTP1B in complex with compound **4** (orthorhombic space group, one dimer per AU) was solved by molecular replacement using AMORE and the coordinates from the refined structure of PTP1B in complex with compound **3** (crystallographic dimer). Refinement was

carried out as described for the complex with compound **3**. For all the other complexes (orthorhombic space group), the position of the bound ligand was identified by difference Fourier maps, using the coordinates of the refined compound **4**-containing complex, without ligand or bound waters. The refinement of all complexes was carried out as described for the PTP1B/compound **3** complex. Statistics for all refined models are listed in Table 2.

The coordinates and structure factors for the six structures described here have been deposited with the Protein Data Bank, accession code 1Q6J, 1Q6M, 1Q6N, 1Q6P, 1Q6S, and 1Q6T, respectively.

RESULTS AND DISCUSSION

Binding Mode for the Aryldifluoromethyl-Phosphonic Acid Inhibitors. All inhibitors reported here bind in a very similar fashion. Compound **2** was the initial compound in the series; hence, we will use the complex of PTP1B/compound **2** (Table 3) for the general description of the binding mode of this class of compounds, and address specific differences in separate paragraphs. These compounds (referred to as benzotriazoles because of the presence of a benzotriazole ring bound to the central, tetra-substituted carbon atom) were designed so that the group at R2 would reach into and take advantage of the secondary phospho-aryl binding site previously described (17). We found that tetra-substituted benzotriazoles are in fact very potent against PTP1B (Table 3), in accord with the theory that utilizing both primary and secondary binding sites would increase affinity by several orders of magnitude (11). These compounds also display a very high degree of selectivity for PTP1B over a variety of other phosphatases (see Table 4).

The structure of PTP1B, both uninhibited and in complex with a variety of substrates/inhibitors, has been previously

made with protein atoms, are very similar to that of the phosphotyrosine (pTyr) bound into the primary binding site in 1PTY.

The second F₂PMP extends toward the secondary binding region, but it does not fully occupy this site. The phenyl ring occupies the position taken by the C α of the second pY in 1PTY, in a hydrophobic cradle formed by the side chains of Val42, Asp48 (CB), and Ile219. The CF₂PO₃ moiety overlaps the phenyl ring of the pTyr of 1PTY. There is an extensive network of 11 ordered solvent molecules that provide a connection between this phosphonate and the main- and side-chain atoms of residues that make up the secondary binding site (Figure 2). From the structures, it appears that the F₂PMP bound in the primary binding site and the benzotriazole function as anchors, locking the inhibitor into place such that substituents at R2 (Table 3) reach into the secondary binding site. Compound **4** is still quite potent and shows a 350-fold improvement in potency compared to an analogue without a substituent in the corresponding position (Table 3). The structure of its complex shows that the cinnamyl group occupies the same site as the difluoromethylene-benzene of compound **2**. This observation suggests that hydrophobic interactions between an aromatic/aliphatic substituent and the hydrophobic cradle formed by the side chains of Val42, Asp48 (C β), and Ile219 probably account for the larger part of the increase in potency observed when a substituent is added at R2 (Table 3).

The benzotriazole moiety is located under the YRD loop. It makes one hydrogen bond with the main chain nitrogen of Asp48, and van der Waals interactions with the side chain of Arg49 (the average distance is 4.5 Å). The interactions involving the benzotriazole moiety with the YRD loop suggest that this class of inhibitors should be fairly selective against other PTPases (27). To assess the selectivity of the nonpeptidic, bisphosphonate PTP1B inhibitors we tested compound **2** as a representative benzotriazole compound on six other protein tyrosine phosphatases including the dual-specificity cdc25 (Table 4). The inhibitor binds strongly to both PTP1B and TCPTP (11–15 nM) and binds at least 2 orders of magnitude more weakly to the other protein tyrosine phosphatases. The closest PTP with respect to binding strength is SHP-1 where the inhibitor is 380 times less potent than on PTP1B. The selectivity over CD45, PTP β , and the dual specificity phosphatase cdc25, which is capable of dephosphorylating Tyr as well as phosphorylated Ser and Thr residues, was quite remarkable at greater than 3000-fold.

The fourth substituent of the central carbon atom, the benzene ring, occupies an area of the binding site that is not occupied by any of the PTP1B ligands whose structures have been reported to date. It lies in a hydrophobic pocket lined by the main- and side-chain atoms of Tyr46, Ser118, and Leu119, and it is located about 3.6 Å away from the side chain of Leu119. The region spanning residues Glu115–Cys121 (orange in Figure 1) is a surface loop that, in the 1PTY structure, is involved in interactions with a symmetry-related molecule, and held in an “open” conformation. In all structures reported here, the different crystal packing scheme leaves this loop fully solvent-exposed and apparently highly mobile. Residues Met114–Leu119 display different conformations in different complexes, but in general the electron density clearly indicates the presence of a “closed”

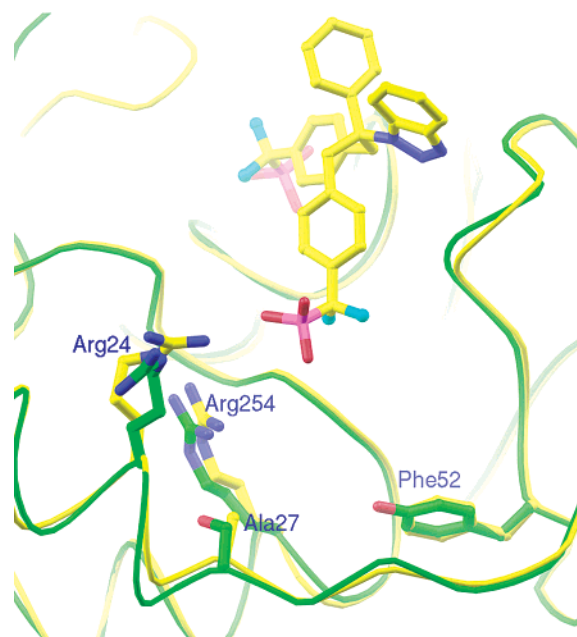
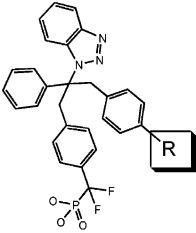
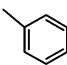
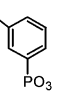
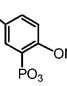
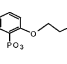
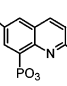
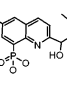
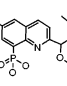
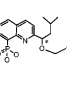


FIGURE 3: The secondary aryl binding site in PTP1B and TCPTP. Ribbon diagram of the secondary aryl binding site in PTP1B (yellow) and TCPTP (green), identified by Arg24 and Arg254. The only differences between PTP1B and TCPTP among the first shell residues are the F52Y and A27S mutations in TCPTP.

conformation that further shields the active site from bulk solvent. In the PTP1B/compound **3** complex the loop is closed, and there are some hydrophobic interactions between residues of the loop and the difluorobenzene. In the PTP1B/compound **2**, **4**, **6**, **9**, and **11** complexes the loop has been modeled in the closed conformation, but the extremely weak electron density, and the very high temperature factors associated with its atoms suggest that the loop probably oscillates between different positions. These observations suggest that the loop position and conformation may depend on the exact chemical nature of the substituent present in the this pocket.

The Design of Selective Inhibitors. Sequence alignment between PTP1B and TCPTP shows that, although the two enzyme share a 72% overall identity, the identity among the residues that make up the catalytic and binding sites is as high as 92%, with only two differences located among the first-shell residues: F52Y and A27S (Figure 3). The recently reported crystal structure TCPTP (15) shows that, as in the PTP1B structure, both residues are located at the far end of the secondary binding site, about 6 Å from the inhibitor second phosphate in the PTP1B/compound **2** complex. Both serine and tyrosine residues have one more atom (the hydroxyl oxygen) respect to the corresponding alanine and phenylalanine in PTP1B, and this change may alter, although by a small amount, the size and the electronic properties of the end of the secondary binding site. On the basis of this idea, several compounds were designed starting from the structural class of compound **2**. The compounds contain, as replacement of the $-\text{CF}_2\text{PO}_3$ moiety, heteroaryl phosphonate fragments that would (a) interact with Arg24 and Arg254, thus providing a way to anchor the compound and possibly increase inhibitor potency, and (b) direct a substituent (R) toward Phe52 and Ala27, thus providing selectivity for PTP1B over TCPTP (Lau et al., in preparation). Table 5 shows several of the compounds synthesized following this

Table 5: IC₅₀ (nM) and Selectivity Ratios for Some of the Compounds Designed to Interact with F52 and A27


R	Compound	PTP1B	TCPTP	TCPTP/PTP1B
	5	38	24	0.6
	6	3	3	1.0
	7	10	31	3.1
	8	6	20	3.5
	9	12	20	1.7
	10	6	17	3.4
	11	5	36	7.2
	12	11	21	1.9

template: as predicted, there is a moderate increase in selectivity that roughly correlates with the size of R, in accord with the fact that the secondary binding site in TCPTP is slightly smaller because of the F52Y and A27S substitutions. Although the absolute selectivity we have achieved in these early compounds is modest, the results are a clear indication that this structure-guided approach to the secondary aryl-binding site is a productive path to achieving selectivity between PTP1B and TCPTP.

The Atomic Basis for Selectivity. To provide a structural explanation for the affinity and selectivity observed with this class of compounds, the structures of PTP1B in complex with compounds **6**, **9**, and **11** have been solved and refined to atomic resolution. Table 2 reports statistics for all refined complexes, and Figure 4 presents stereoviews of the three compounds bound to PTP1B. All the structures of the second generation inhibitors were solved in the orthorhombic system, with two molecules per asymmetric unit. In general, the two molecules are virtually identical except for rotations of surface side chains and the position of the loop spanning

residues Glu115-Cys121. Compound **6** is the smallest in the series, and does not display any selectivity. As predicted by modeling, it is hydrogen bonded through the phosphate to the side chains of Arg24 and Arg254 (Figure 4A). The aromatic ring is about 7 Å from the side chain of Phe52, and 6.5 Å from Ala27, too far to interact with these residues or with their larger replacements (Tyr54 and Ser29) in TCPTP. Unlike the other compounds in this series, compound **6** assumes two distinct conformations in the two molecules (Figure 4A). In the second conformation, the arylphosphonate is rotated so that the phosphate is fully solvent exposed. Although in this second conformation, the distances between the arylphosphonate and the side chains of Phe52 and Ala27 are similar to those observed in the other conformer, the presence of two distinct species suggests that this structural class is intrinsically very flexible and, as such, not a good template for the design of optimized compounds.

Compounds **9** and **11** are quinoline phosphonic acid analogues: this aromatic system provides a much more rigid scaffold, and only one conformation for the compound is observed in the crystal structures. Compound **9** shows limited selectivity (1.7×) consistent with the distances between the methyl and the side chains of Phe52 and Ala27 (4.8 and 6.1 Å, respectively, Figure 4B). Compound **11** (Lau et al., in preparation) shows moderate selectivity (7.2×), consistent with the proximity (3.7 Å) of its methoxy group and the side chain of Phe52. The compound is still quite far away from Ala27, and from these crystal structures it appears that the pocket containing Phe52 is a more accessible area for the design of selective inhibitors than the region of Ala27.

To confirm the finding that the F52Y substitution is indeed the responsible for the difference in affinity observed for the two enzymes in this class of compounds, the PTP1B F52Y and TCPTP Y54F were constructed and assayed against compounds **11**, **13** (a much less potent diastereoisomer of **11**), and **14** (a nanomolar inhibitor of PTP1B that is known not to bind into the secondary binding site (21)). Table 6 shows the affinities of these compounds for the WT and mutant enzymes. The affinity of compound **14** is essentially identical for both enzymes, and it binds equally well to both mutant proteins, consistent with the fact that it does not interact with the secondary aryl-binding site. Compound **11** is about 6-fold more potent on WT-PTP1B than WT-TCPTP, and the affinity for the PTP1B F52Y mutant is decreased by about 6-fold, while the affinity for the TCPTP Y54F mutant is about 3-fold higher than the affinity for the WT-TCPTP. These results suggest that the compound is indeed interacting with the side chain of Phe52, and that the generally conservative phenylalanine to tyrosine mutation is responsible for most of the observed selectivity of this inhibitor. Interestingly, the much less potent compound **13**, the diastereoisomer isomeric at the methine (Table 6), follows the same trend, indicating that the quinoline phosphonic acid analogue is still binding into the secondary aryl phosphate binding site. The different stereochemistry at the methine is accommodated by switching the position of the benzotriazole and the phenol-groups.

CONCLUSIONS

PTP1B, the best-characterized member of the protein tyrosine phosphatase family, has been implicated in the

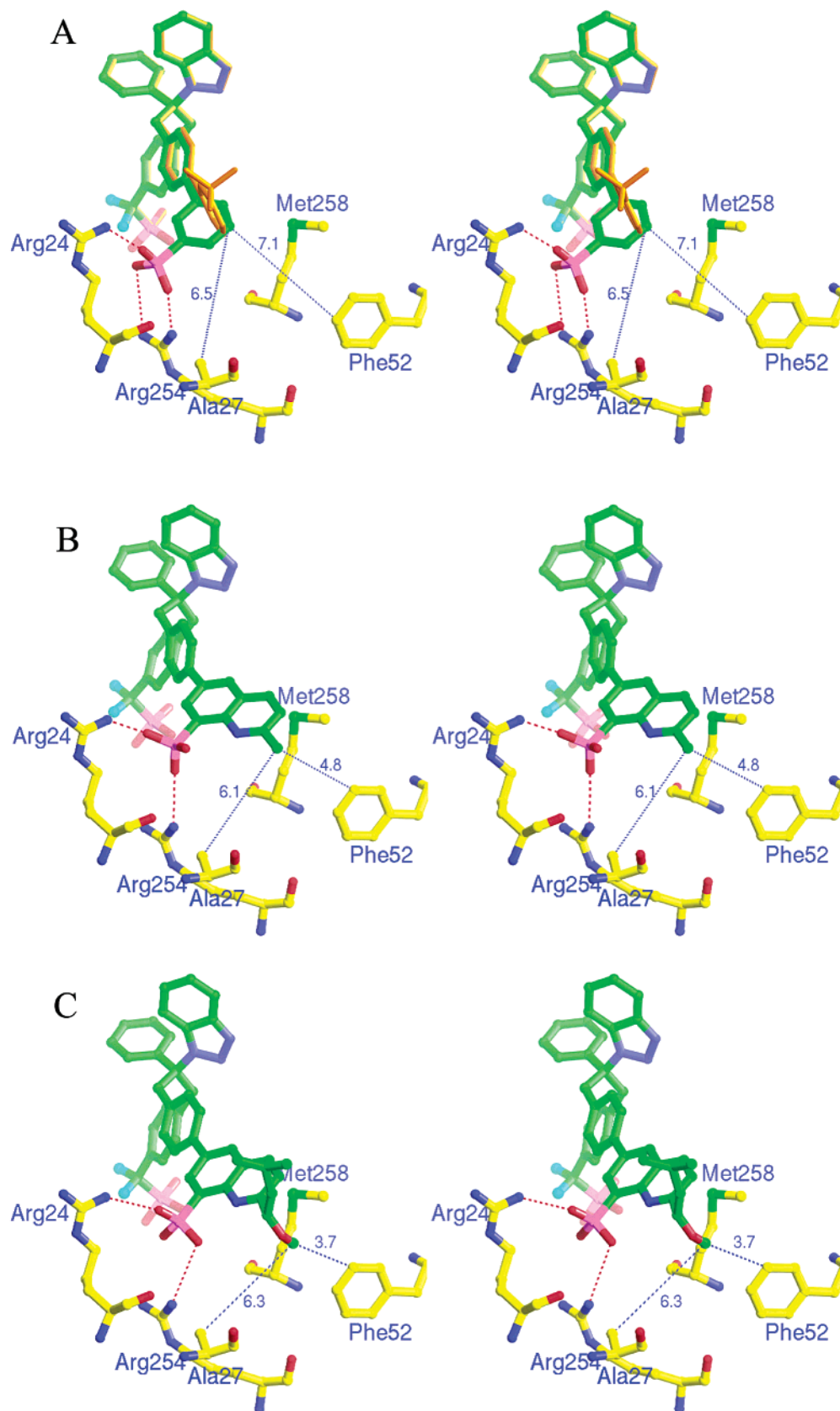
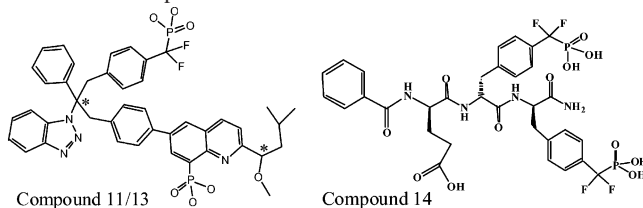


FIGURE 4: Interactions of the second-generation compounds with the secondary aryl-binding site. Stereoviews of (A) compound **6**, (B) compound **9**, and (C) compound **11** bound into the PTP1B secondary aryl-binding site. The hydrogen bond interactions with the side-chains of R24 and R254 are indicated by red dotted lines. The distance between the bound compounds and the side chains of Phe52 and Ala27 are indicated by blue dotted lines. In panel A, the alternate conformation for compound **6** is displayed as orange sticks.

regulation of the insulin signaling pathway and represents an attractive target for the design of inhibitors in the treatment

of type 2 diabetes and obesity. We report here the structures of PTP1B in complex with first and second generation

Table 6: Affinity (IC_{50} , nM) of Compounds **11**, **13**, and **14** for WT and Mutant Phosphatases


	compound 11	compound 13	compound 14
PTP1B WT	7 ± 2	148 ± 30	5 ± 3
PTP1B F52Y	38 ± 5	372 ± 20	7 ± 2
TCPTP WT	44 ± 6	444 ± 70	8 ± 3
TCPTP Y54F	17 ± 3	195 ± 35	8 ± 2

members of a new class of potent and selective inhibitors. The crystallographic analysis shows that the second generation inhibitors bind into the secondary binding site, and points to Phe52 as potential determinant for the selectivity displayed by these compounds for PTP1B over the highly homologous TCPTP. Mutagenesis data confirm these findings, and further indicate that the pocket containing Phe52 is an accessible area for the design of selective inhibitors. In addition, novel interactions with residues of the phosphotyrosine recognition loop (43–48) and residues of the loop spanning residues 114–118 have been identified. These structures and compounds thus provide a novel and promising framework for the design of inhibitors that address the potency and selectivity issues associated with PTP1B inhibition.

ACKNOWLEDGMENT

We thank Dr. Kathleen Metters for her continued support, and the staff at the facilities at the Industrial Macromolecular Crystallography Association Collaborative Access Team (IMCA-CAT) for help during data collection.

REFERENCES

- Fisher, E. H., Charbonneau, H., and Tonks, N. K. (1991) Protein tyrosine phosphatases: a diverse family of intracellular and transmembrane enzymes. *Science* 253, 401–406.
- Hunter, T. (1995) Protein kinases and phosphatases: the yin and yang of protein phosphorylation and signaling. *Cell* 80, 225–236.
- Barford, D. (1995) Protein Phosphatases. *Curr. Opin. Struct. Biol.* 5, 728–734.
- Neel, B. G., and Tonks, N. K. (1997) Protein tyrosine phosphatases in signal transduction. *Curr. Opin. Cell. Biol.* 9, 193–204.
- Tonks, N. K., Diltz, C. D., and Fisher, E. H. (1988) Purification of the major protein tyrosine phosphatases from human placenta. *J. Biol. Chem.* 263, 6722–6730.
- Tonks, N. K., Diltz, C. D., and Fisher, E. H. (1988) Characterization of the major protein tyrosine phosphatases from human placenta. *J. Biol. Chem.* 263, 6731–6737.
- Barford, D., Flint, A. J., and Tonks, N. K. (1994) Crystal Structure of Human Protein Tyrosine Phosphatase 1B. *Science* 263, 1397–1404.
- Elchebly, M., Payette, P., Michaliszyn, E., Cromlish, W., Collins, S., Loy, A. L., Normandin, D., Cheng, A., Himms-Hagen, J., Chan, C.-C., Ramachandran, C., Gresser, M. J., Tremblay, M. L., and Kennedy, B. P. (1999) Increased insulin sensitivity and obesity resistance in mice lacking the protein tyrosine phosphatase 1B gene. *Science* 283, 1544–1548.
- Klaman, L. D., Boss, O., Peroni, O. D., Kim, J. K., Martino, J. L., Zabolotny, J. M., Moghal, N., Lubkin, M., Kim, Y. B., Sharpe, A. H., Stricker-Krongrad, A., Shulman, G. I., Neel, B. G., and

- Kahn, B. B. (2000) Increased energy expenditure, decreased adiposity, and tissue-specific insulin sensitivity in protein-tyrosine phosphatase 1B-deficient mice. *Mol. Cell. Biol.* 20, 5479–5489.
- Ukkola, O., and Santaniemi, M. (2002) Protein tyrosine phosphatase 1B: a new target for the treatment of obesity and associated co-morbidities. *J. Intern. Med.* 251, 467–475.
- Zhang, Z. Y. (2002) Protein tyrosine phosphatases: Structure and function, substrate specificity, and inhibitor development. *Annu. Rev. Pharmacol. Toxicol.* 42, 209–234.
- Blaskovich, M. A., and Kim, H. O. (2002) Recent discovery and development of protein tyrosine phosphatase inhibitors. *Exp. Opin. Ther. Pat.* 12, 871–905.
- Tonks, N. K. (2003) PTP1B: From the sidelines to the front lines! *FEBS Lett.* 546, 140–148.
- Cool, D. E., Tonks, N. K., Charbonneau, H., Walsh, K. A., Fisher, E. H., and Krebs, E. G. (1989) cDNA isolated from a human T-cell library encodes a member of the protein tyrosine phosphatase family. *Proc. Natl. Acad. Sci. U.S.A.* 86, 5257–5261.
- Iversen, L. F., Moller, K. B., Pedersen, A. K., Peters, G. H., Petersen, A. S., Andersen, H. S., Branner, S., Mortensen, S. B., and Moller, N. P. (2002) Structure determination of T cell protein-tyrosine phosphatase. *J. Biol. Chem.* 277, 19982–19990.
- You-Ten, K. E., Muise, E. S., Itié, A., Michaliszyn, E., Wagner, J., Jothy, S., Lapp, W. S., and Tremblay, M. L. (1997) Impaired bone marrow microenvironment and immune function in T cell protein tyrosine phosphatase-deficient mice. *J. Exp. Med.* 186, 683–693.
- Puius, Y. A., Zhao, Y., Sullivan, M., Lawrence, D. S., Almo, S. C., and Zhang, Z.-Y. (1997) Identification of a second aryl phosphate-binding site in protein tyrosine-phosphatase 1B: a paradigm for inhibitor design. *Proc. Nat. Acad. Sci., U.S.A.* 94, 13420–13425.
- Salmeen, A., Andersen, J. N., Meyers, M. P., Tonks, N. K., and Barford, D. (2000) Molecular Basis for dephosphorylation of the active segment of the insulin receptor by protein tyrosine phosphatase 1B. *Mol. Cell* 6, 1401–1412.
- Jia, Z., Ye, Q., Dinaut, A. N., Wang, Q., Waddleton, D., Payette, P., Ramachandran, C., Kennedy, B., Hum, G., and Taylor, S. D. (2001) Structure of Protein Tyrosine Phosphatase 1B in Complex with Inhibitors Bearing Two Phosphotyrosine Mimetics. *J. Med. Chem.* 44, 4584–4594.
- Shen, K., Keng, Y.-F., Wu, L., Guo, X.-L., Lawrence, D. S., and Zhang, Z.-Y. (2001) Acquisition of a Specific and Potent PTP1B Inhibitor from a Novel Combinatorial Library and Screening Procedure. *J. Biol. Chem.* 276, 47311–47319.
- Asante-Appiah, E., Patel, S., Dufresne, C., Roy, P., Wang, Q., Patel, V., Friesen, R. W., Ramachandran, C., Becker, J. W., Leblanc, Y., Kennedy, B. P., and Scapin, G. (2002) The structure of PTP-1b in complex with a peptide inhibitor reveals an alternative binding mode for bisphosphonates. *Biochemistry* 41, 9043–9051.
- Sun, J.-P., Fedorov, A. A., Lee, S.-Y., Guo, X.-L., Shen, Lawrence, D. S., Almo, S. C., and Zhang, Z.-Y. (2003) Crystal Structure of PTP1B Complexed with a Potent and Selective Bidentate Inhibitor. *J. Biol. Chem.* 278, 12406–12414.
- Szczepankiewicz, B. G., Liu, G., Hajduk, P. J., Abad-Zapatero, C., Pei, Z., Xin, Z., Lubben, T. H., Trevillyan, J. M., Stashko, M. A., Ballaron, S. J., Liang, H., Huang, F., Hutchins, C. W., Fesik, S. W., and Jirousek, M. R. (2003) Discovery of a Potent, Selective Protein Tyrosine Phosphatase 1B Inhibitor Using a Linked-Fragment Strategy. *J. Am. Chem. Soc.* 125, 4087–4096.
- Xin, Z., Oost, T. K., Abad-Zapatero, C., Hajduk, P. J., Pei, Z., Szczepankiewicz, B. G., Hutchins, C. W., Ballaron, S. J., Stashko, M. A., Lubben, T., Trevillyan, J. M., Jirousek, M. R., and Liu, G. (2003) Potent, selective inhibitors of protein tyrosine phosphatase 1B. *Bioorg. Med. Chem. Lett.* 13, 1887–1890.
- Romsicki, Y., Kennedy, B. P., and Asante-Appiah, E. (2003) Purification and characterization of T Cell protein tyrosine phosphatase reveals significant functional homology to protein tyrosine phosphatase-1B. *Arch. Biochem. Biophys.* 414, 40–50.
- Ausubel, F. M., Brent, R., Kingston, R. E., Moore, D. D., Seidman, J. G., Smith, J. A., and Struhl, K. (1992) *Short Protocols in Molecular Biology*, Green Publishing Associates/John Wiley and Sons, Inc., New York.
- Asante-Appiah, E., Ball, K., Bateman, K., Skorey, K., Friesen, R., Despons, C., Payette, P., Bayly, C., Zamboni, R., Scapin, G., Ramachandran, C., and Kennedy, B. P. (2001) The YRD motif is

- a major determinant of substrate and inhibitor specificity in T-cell protein-tyrosine phosphatase. *J. Biol. Chem.* 276, 26036–26043.
28. Huang, Z., Wang, Q., Ly, H. D., Gorvindarajan, A., Scheigetz, J., Zamboni, R., Desmarais, S., and Ramachandran, C. (1999) 3,6-Fluorescein diphosphate: A sensitive fluorogenic and chromogenic substrate for protein tyrosine phosphatases. *J. Biomol. Screening* 4, 327–334.
29. Howard, A. J. (2001) Data processing in Macromolecular Crystallography in *Crystallographic Computing 7: Proceedings from the Macromolecular Crystallographic Computing School, 1996* (Bourne, P. E., and Watenpaugh, K. D., Ed.) Oxford University Press, Oxford.
30. Navaza, J. (1994) AMoRe: an automated package for molecular replacement. *Acta Crystallogr.* 50, 157–163.
31. Brünger, A. T., Kuriyan, J., and Karplus, M. (1987) Crystallographic R-factor refinement by Molecular Dynamics. *Science* 235, 458–460.
32. Brünger, A. T., Krukowski, J., and Erickson, J. (1990) Slow-cooling protocols for crystallographic refinement by simulated annealing. *Acta Crystallogr. A* 46, 585–593.
33. Brünger, A. T. (1992) The free-R value: a novel statistical quantity for assessing the accuracy of crystal structures. *Nature* 355, 472–474.
34. Rice, L. M., and Brunger, A. T. (1994) Torsion Angle Dynamics: Reduced Variable Conformational Sampling Enhances Crystallographic Structure Refinement. *Proteins: Struct. Funct. Genet.* 19, 277–290.
35. Brünger, A. T., Adams, P. D., Clore, G. M., DeLano, W. L., Gros, P., Grosse-Kunstleve, R. W., Jiang, J.-S., Kuszewski, J., Nilges, M., Pannu, N. S., Read, R. J., Rice, L. M., Simonson, T., and Warren, G. L. (1998) *Crystallography & NMR System: a New Software Suite for Macromolecular Structure Determination. Acta Crystallogr. D* 54, 905–921.
36. Andersen, J. N., Mortensen, O. H., Peters, G. H., Drake, P. G., Iversen, L. F., Olsen, O. H., Jansen, P. G., Andersen, H. S., Tonks, N. K., and Moller, N. P. (2001) Structural and Evolutionary Relationships among Protein Tyrosine Phosphatase Domains. *Mol. Cell Biol.* 21, 7117–36.
37. Carson, M. (1997) Ribbons. *Methods Enzymol.* 277, 493–505.

BI035098J